VNU Journal of Science: Mathematics - Physics

Journal homepage: https://js.vnu.edu.vn/MaP

Original Article

Nonlinear Static Stability of Stiffened Nanocomposite Plates Subjected Various Types of Loads

Nguyen Van Thanh*

VNU University of Engineering and Technology, 144 Xuan Thuy, Cau Giay, Hanoi, Vietnam

Received 29 October 2021
Revised 11 November 2021; Accepted 11 November 2021

Abstract: This work deals with the nonlinear buckling and post-buckling of stiffened nanocomposite plates reinforced functionally graded carbon nanotubes (FG CNTRC) resting on elastic foundation in thermal environment. Obtained results showed that the properties of the nanocomposited plates embedded with single-walled carbon nanotubes are dependent on temperature and altered according to linear functions of the thickness. The governing equations are derived by the third-order shear deformation plate theory taking into account von Kármàn geometrical nonlinearity and solved by both the Airy's stress function and Galerkin method. In numerical results, the influences of various types of distribution and volume fractions of carbon nanotubes, geometrical parameters, elastic foundations on the nonlinear buckling and post-buckling behaviour of stiffened FG-CNTC plates subjected mechanical, thermal loading and both are demonstrated.

Keywords: Stiffened FG CNTRC plates; Buckling and Post buckling analysis; Third-order shear deformation theory; Thermal environment; Galerkin method.

1. Introduction

Carbon nanotubes (CNTs) were first discovered by Sumio Iijima in 1991 which have valuable properties such as incredible strength, lightweight, super-high stiffness, unique electrical properties and thermal conductivity [1-5]. CNTs are the ideal reinforcement material for a variety of new composites with metal, polymer, rubber, epoxy matrices. Therefore, there are many proposed papers of applying CNTs on the nanocomposite plates to investigate the buckling and post-buckling behaviour.

* Corresponding author.
E-mail address: nguyenvanthanh8583@gmail.com

https//doi.org/10.25073/2588-1124/vnumap.4685

Shen [6] first presented the nonlinear bending behaviour of functionally graded carbon nanotubes (FG-CNT) reinforced composite plates in thermal environments. After that, Shen and Zhu [7] presented the results of buckling and post-buckling behaviour of FG-CNT reinforced composite plates in thermal environment based on a third-order shear deformation plate theory (TSDT) and taking the von Kármán's geometrical nonlinearity into account. Using the first-order shear deformation theory (FSDT), Kiani presented the shear buckling behaviours [8] and the thermal post-buckling behaviours [9] of FG-CNT reinforced composite plates in the thermal environment subjected to uniform temperature rise loading; Zhang et al., [10-11] applied the element-free approach to investigate the buckling and post-buckling behaviours of FG-CNT reinforced composite plates resting on Pasternak's elastic foundation; The FG-X type of CNTs reinforced the composite plates has the highest critical mechanical and thermal buckling load reported by Mizaei and Kiani [12-13].

Stiffeners are often used to increase the load carrying capacity and avoid instability of the structure. There are some results of the buckling and post-buckling behaviours and vibration for stiffened composite structures. Duc et al., [14] presented the analytical solutions to study nonlinear buckling behaviours of imperfect stiffened composite cylindrical panels reinforced by CNTs resting on elastic foundations in thermal environments. Avramov et al., [15] presented the mathematical model of transient response of functionally graded carbon nanotubes reinforced conical shell with ring-stiffeners based on the TSDT. Maji et al., [16] studied the thermo-elastic vibration of graphene reinforced composite stiffened plate with general boundary conditions using FEM based on first-order shear deformation theory. Davar et al., [17-18] presented the dynamic response and free vibration of a grid-stiffened composite cylindrical shell reinforced by CNTs subjected to the radial impulse load. Bo et al. [19] investigated the nonlinear dynamic investigation of the perovskite solar cell with GPLR-FGP stiffeners under blast impact based on the von-Kármán geometric nonlinearity and the first-order shear deformation theory. Fu et al., [20] applied the analytical approach for sound transmission through stiffened double laminated composite sandwich plates. Bakshi [21] presented the nonlinear vibrations of laminated composite singly curved stiffened shells using FEM. Liu et al., [22] developed the unified method for the vibration analysis of stiffened plate subjected to moving loads traveling along arbitrary paths.

This paper presents the buckling and post-buckling behaviours of stiffened nanocomposite plates reinforced by FG-CNTs subjected to mechanical, thermal loading and both. The results obtained from buckling and post-buckling analysis of FG CNTRC plates using the analytical method will support scientific foundations for structural designers, manufacturers and for building projects for FG CNTRC structures. Our aim is to study an analytical approach to obtain the mechanical and thermal buckling and post-buckling behaviours of stiffened nanocomposite plates based on the third-order shear deformation plate theory.

2. Material Properties

The effective mechanical properties of FG CNTRC plates are estimated by the extended rule of mixture as follows [6]:

$$\begin{aligned} E_{11} &= \eta_1 V_{CNT} E_{11}^{CNT} + V_m E_m, \\ \frac{\eta_2}{E_{22}} &= \frac{V_{CNT}}{E_{22}^{CNT}} + \frac{V_m}{E_m}, \\ \frac{\eta_3}{G_{12}} &= \frac{V_{CNT}}{G_{12}^{CNT}} + \frac{V_m}{G_m}, \end{aligned} \tag{1}$$

where E_{11}^{CNT}, E_{11}^{CNT}, G_{12}^{CNT} are the Young and shear moduli of (10,10) single-walled carbon nanotubes (SWCNTs) with values $E_{11}^{CNT} = 5.6466\,(TPa)$, $E_{22}^{CNT} = 7.08\,(TPa)$, $G_{12}^{CNT} = 1.9445\,(TPa)$ and also $\nu_{12}^{CNT} = 0.175$. The nanocomposites are considered to be embedded in the amorphous polymer matrix Poly Methyl Methacrylate (PMMA) with the elastic modulus and Poisson's ratio are $E_m = (3.52 - 0.0034T)\,GPa, \alpha_m = 45\left(1 + 0.0005\Delta T\right)\times 10^{-6}\,/\,K, \nu_m = 0.34$. The efficiency parameters $\eta_i\,(i = \overline{1,3})$ calculated by molecular dynamics simulation have been shown in Table 1 [6-7].

Table 1. Efficiency parameters for CNT reinforced composite plates (after [6, 7])

V_{CNT}^*	η_1	η_2	η_3
0.12	0.137	1.022	0.715
0.17	0.142	1.626	1.138
0.28	0.141	1.585	1.110

Poisson's ratio (v_{12}) and thermal expansion (α_{11}, α_{22}) are calculated as:

$$v_{12} = V_{CNT}^* v_{12}^{CNT} + V_m v_m, \tag{2}$$

$$\begin{aligned} \alpha_{11} &= \frac{V_m E_m \alpha_m + V_{CNT} E_{11}^{CNT} \alpha_{11}^{CNT}}{V_m E_m + V_{CNT} E_{11}^{CNT}}, \\ \alpha_{22} &= \left(1 + v_m\right) V_m \alpha_m + \left(1 + v_{12}^{CNT}\right) V_{CNT} \alpha_{22}^{CNT} - v_{12}\alpha_{11}. \end{aligned} \tag{3}$$

where, V_{CNT}, $\nu_{12}^{CNT}, \alpha_{11}^{CNT}, \alpha_{22}^{CNT}$ and V_m, ν_m, α_m are the volume fractions, Poisson's ratios and thermal expansion of CNTs and the polymer matrix, respectively.

The FG CNTRC materials were made by various polymer matrices reinforced by (10,10) SWCNTs which are assumed to be graded through the thickness direction of the plates. Three types of CNT's distribution are considered: uniform distribution (UD) and two types of functionally graded distribution of CNTs (FG-X and FG-O) having maximum volume fraction: i) At the upper and lower external surfaces of the plate; and ii) at the mid height of the plate thickness respectively.

$$\begin{cases} V_{CNT} = V_{CNT}^* & \text{UD} \\ V_{CNT} = 4\dfrac{|z|}{h^k} V_{CNT}^* & \text{FG-X} \\ V_{CNT} = 2\left(1 - 2\dfrac{|z|}{h^k}\right) V_{CNT}^* & \text{FG-O} \end{cases} \tag{4}$$

3. Theoretical Formulations

Consider a FG CNTRC plate with length of edges a, b, and thickness h, s_1, s_2 are spacing of the longitudinal and transversal stiffeners, respectively; z_1, z_2 are the eccentricities of stieners with respect to the middle surface of plate, respectively; d_1, h_1 and d_2, h_2 are the width and thickness of longitudinal and transversal stieners, respectively. A coordinate system (x, y, z) is derived in which (x, y) plane on the middle surface of the shell and z on thickness direction $(-h/2 \le z \le h/2)$ as shown in Figure 1.

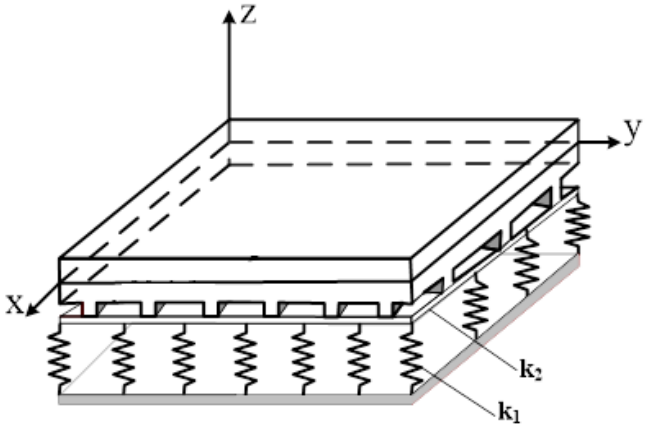

Figure 1. A plate resting on elastic foundations.

The governing equations of nanocomposite plates reinforced by CNTs are derived by TSDT. The strain components taking into account von Kármàn nonlinear terms are given by [24]:

$$\begin{pmatrix}\varepsilon_x\\ \varepsilon_y\\ \gamma_{xy}\end{pmatrix}=\begin{pmatrix}\varepsilon_x^0\\ \varepsilon_y^0\\ \gamma_{xy}^0\end{pmatrix}+z\begin{pmatrix}k_x^1\\ k_y^1\\ k_{xy}^1\end{pmatrix}+z^3\begin{pmatrix}k_x^3\\ k_y^3\\ k_{xy}^3\end{pmatrix};\begin{pmatrix}\gamma_{xz}\\ \gamma_{yz}\end{pmatrix}=\begin{pmatrix}\gamma_{xz}^0\\ \gamma_{yz}^0\end{pmatrix}+z^2\begin{pmatrix}k_{xz}^2\\ k_{yz}^2\end{pmatrix}, \tag{5}$$

with

$$\begin{pmatrix}\varepsilon_x^0\\ \varepsilon_y^0\\ \gamma_{xy}^0\end{pmatrix}=\begin{pmatrix}\dfrac{\partial u}{\partial x}+\dfrac{1}{2}\left(\dfrac{\partial w}{\partial x}\right)^2\\ \dfrac{\partial v}{\partial y}+\dfrac{1}{2}\left(\dfrac{\partial w}{\partial y}\right)^2\\ \dfrac{\partial u}{\partial y}+\dfrac{\partial v}{\partial x}+\dfrac{\partial w}{\partial x}\dfrac{\partial w}{\partial y}\end{pmatrix},\begin{pmatrix}k_x^1\\ k_y^1\\ k_{xy}^1\end{pmatrix}=\begin{pmatrix}\dfrac{\partial \phi_x}{\partial x}\\ \dfrac{\partial \phi_y}{\partial y}\\ \dfrac{\partial \phi_x}{\partial y}+\dfrac{\partial \phi_y}{\partial x}\end{pmatrix},\begin{pmatrix}k_x^3\\ k_y^3\\ k_{xy}^3\end{pmatrix}=-c_1\begin{pmatrix}\dfrac{\partial \phi_x}{\partial x}+\dfrac{\partial^2 w}{\partial x^2}\\ \dfrac{\partial \phi_y}{\partial y}+\dfrac{\partial^2 \mathrm{w}}{\partial y^2}\\ \dfrac{\partial \phi_x}{\partial y}+\dfrac{\partial \phi_y}{\partial x}+2\dfrac{\partial^2 \mathrm{w}}{\partial x\partial y}\end{pmatrix}$$
$$\begin{pmatrix}k_{xz}^2\\ k_{yz}^2\end{pmatrix}=-3c_1\begin{pmatrix}\phi_x+\dfrac{\partial \mathrm{w}}{\partial x}\\ \phi_y+\dfrac{\partial \mathrm{w}}{\partial y}\end{pmatrix},\begin{pmatrix}\gamma_{xz}^0\\ \gamma_{yz}^0\end{pmatrix}=\begin{pmatrix}\phi_x+\dfrac{\partial \mathrm{w}}{\partial x}\\ \phi_y+\dfrac{\partial \mathrm{w}}{\partial y}\end{pmatrix},c_1=4/3h^2,c_2=3c_1. \tag{6}$$

The strain-stress relations are defined as [24]:

$$\begin{bmatrix} \sigma_x \\ \sigma_y \\ \sigma_{yz} \\ \sigma_{xz} \\ \sigma_{xy} \end{bmatrix} = \begin{bmatrix} Q_{11} & Q_{12} & 0 & 0 & 0 \\ Q_{12} & Q_{22} & 0 & 0 & 0 \\ 0 & 0 & Q_{44} & 0 & 0 \\ 0 & 0 & 0 & Q_{55} & 0 \\ 0 & 0 & 0 & 0 & Q_{66} \end{bmatrix} \begin{bmatrix} \varepsilon_x - \alpha_{11}\Delta T \\ \varepsilon_y - \alpha_{22}\Delta T \\ \gamma_{yz} \\ \gamma_{xz} \\ \gamma_{xy} \end{bmatrix}, \tag{7}$$

where:

$$Q_{11} = \frac{E_{11}}{1-\nu_{12}\nu_{21}}, Q_{22} = \frac{E_{22}}{1-\nu_{12}\nu_{21}}, Q_{12} = \frac{\nu_{21}E_{11}}{1-\nu_{12}\nu_{21}}, Q_{44} = G_{23} = 1,2G_{12}, Q_{55} = G_{13} = G_{12}, Q_{66} = G_{12}. \tag{8}$$

and for stiffeners:

$$\begin{pmatrix} \sigma_x^s \\ \sigma_y^s \end{pmatrix} = E_0 \begin{pmatrix} \varepsilon_x \\ \varepsilon_y \end{pmatrix} - \frac{1}{1-2v_0} E_0 \alpha_0 \Delta T \tag{9}$$

The force and moment components can be given by:

$$\begin{aligned} \left(N_i, M_i, P_i\right) &= \int_{-h/2}^{h/2} \sigma_i(1, z, z^3)dz + \int_{-h/2-h_i}^{-h/2} \sigma_i^s(1, z, z^3).\frac{d_i^t}{s_i^t}dz,\ i = x, y \\ \left(N_{xy}, M_{xy}, P_{xy}\right) &= \int_{-h/2}^{h/2} \sigma_{xy}(1, z, z^3)dz \\ \left(Q_i, R_i\right) &= \int_{-h/2}^{h/2} \sigma_{iz}(1, z^2)dz,\ i = x, y. \end{aligned} \tag{10}$$

The force and moment results are obtained by Eq. (10) in terms of the stress components as:

$$\begin{aligned} N_x &= B_{11}\varepsilon_x^0 + B_{12}\varepsilon_y^0 + B_{13}k_x^1 + B_{14}k_y^1 + B_{15}k_x^3 + B_{16}k_y^3 - B_{17}\Phi_1 - B_{18}\Phi_{1x}^s, \\ N_y &= B_{12}\varepsilon_x^0 + B_{22}\varepsilon_y^0 + B_{24}k_y^1 + B_{14}k_x^1 + B_{16}k_x^3 + B_{26}k_y^3 - B_{17}\Phi_2 - B_{28}\Phi_{1y}^s, \\ N_{xy} &= B_{31}\gamma_{xy}^0 + B_{32}k_{xy}^1 + B_{33}k_{xy}^3, \\ M_x &= B_{13}\varepsilon_x^0 + B_{14}\varepsilon_y^0 + B_{43}k_x^1 + B_{44}k_y^1 + B_{45}k_x^3 + B_{46}k_y^3 - B_{17}\Phi_3 - B_{18}\Phi_{2x}^s, \\ M_y &= B_{14}\varepsilon_x^0 + B_{24}\varepsilon_y^0 + B_{44}k_x^1 + B_{54}k_y^1 + B_{46}k_x^3 + B_{56}k_y^3 - B_{17}\Phi_4 - B_{28}\Phi_{2y}^s, \\ M_{xy} &= B_{32}\gamma_{xy}^0 + B_{62}k_{xy}^1 + B_{63}k_{xy}^3, \\ P_x &= B_{71}\varepsilon_x^0 + B_{16}\varepsilon_y^0 + B_{73}k_x^1 + B_{46}k_y^1 + B_{75}k_x^3 + B_{76}k_y^3 - B_{17}\Phi_5 - B_{18}\Phi_{4x}^s, \\ P_y &= B_{16}\varepsilon_x^0 + B_{82}\varepsilon_y^0 + B_{46}k_x^1 + B_{84}k_y^1 + B_{76}k_x^3 + B_{86}k_y^3 - B_{17}\Phi_6 - B_{28}\Phi_{4y}^s, \\ P_{xy} &= B_{33}\gamma_{xy}^0 + B_{63}k_{xy}^1 + B_{93}k_{xy}^3, \\ Q_x &= B_{31}\gamma_{xz}^0 + B_{62}k_{xz}^2, \\ Q_y &= 1,2.B_{31}\gamma_{yz}^0 + 1,2.B_{62}k_{yz}^2, \\ R_x &= B_{62}\gamma_{xz}^0 + B_{63}k_{xz}^2, \end{aligned} \tag{11}$$

$$R_y = 1,2.B_{62}\gamma_{yz}^0 + 1.2.B_{63}k_{yz}^2,$$

with $B_{ij}\,(i,j=1\div 8)$ are given in Appendix

The nonlinear strain fields $\varepsilon_x^0, \varepsilon_y^0, \gamma_{xy}^0$ in Eq. (11) can be expressed as :

$$\begin{aligned}
\varepsilon_x^0 &= \frac{B_{22}}{\Delta}N_x - \frac{B_{12}}{\Delta}N_y - \frac{B_{13}B_{22}-B_{14}B_{12}}{\Delta}k_x^1 - \frac{B_{14}B_{22}-B_{24}B_{12}}{\Delta}k_y^1 - \frac{B_{15}B_{22}-B_{16}B_{12}}{\Delta}k_x^3 \\
&- \frac{B_{16}B_{22}-B_{26}B_{12}}{\Delta}k_y^3 - \frac{B_{12}B_{17}\Phi_2 - B_{22}B_{17}\Phi_1}{\Delta} - \frac{B_{28}B_{12}}{\Delta}\Phi_{1y}^s + \frac{B_{18}B_{22}}{\Delta}\Phi_{1x}^s \\
\varepsilon_y^0 &= \frac{B_{11}}{\Delta}N_y - \frac{B_{12}}{\Delta}N_x - \frac{B_{11}B_{14}-B_{13}B_{12}}{\Delta}k_x^1 - \frac{B_{11}B_{24}-B_{14}B_{12}}{\Delta}k_y^1 - \frac{B_{11}B_{16}-B_{15}B_{12}}{\Delta}k_x^3 \\
&- \frac{B_{11}B_{26}-B_{16}B_{12}}{\Delta}k_y^3 - \frac{B_{12}B_{17}\Phi_1 - B_{11}B_{17}\Phi_2}{\Delta} - \frac{B_{18}B_{12}}{\Delta}\Phi_{1x}^s + \frac{B_{11}B_{28}}{\Delta}\Phi_{1y}^s \\
\gamma_{xy}^0 &= \frac{1}{B_{31}}N_{xy} - \frac{B_{32}}{B_{31}}k_{xy}^1 - \frac{B_{33}}{B_{31}}k_{xy}^3, \Delta = B_{11}B_{22} - B_{12}^2.
\end{aligned} \tag{12}$$

and Airy's stress function $f(x,y)$ is determined as:

$$N_x = \frac{\partial^2 f}{\partial y^2}, N_y = \frac{\partial^2 f}{\partial x^2}, N_{xy} = -\frac{\partial^2 f}{\partial x \partial y} \tag{13}$$

The nonlinear equilibrium equation of the nanocomposite plates are shown as:

$$\frac{\partial N_x}{\partial x} + \frac{\partial N_{xy}}{\partial y} = 0,\ \frac{\partial N_{xy}}{\partial x} + \frac{\partial N_y}{\partial y} = 0 \tag{14a}$$

$$\begin{aligned}
&\frac{\partial Q_x}{\partial x} + \frac{\partial Q_y}{\partial y} - 3c_1\left(\frac{\partial R_x}{\partial x} + \frac{\partial R_y}{\partial y}\right) + c_1\left(\frac{\partial^2 P_x}{\partial x^2} + 2\frac{\partial^2 P_{xy}}{\partial x \partial y} + \frac{\partial^2 P_y}{\partial y^2}\right) \\
&+ N_x\frac{\partial^2 w}{\partial x^2} + 2N_{xy}\frac{\partial^2 w}{\partial x \partial y} + N_y\frac{\partial^2 w}{\partial y^2} - k_1 w + k_2\nabla^2 w = 0
\end{aligned} \tag{14b}$$

$$\frac{\partial M_x}{\partial x} + \frac{\partial M_{xy}}{\partial y} - Q_x + 3c_1 R_x - c_1\left(\frac{\partial P_x}{\partial x} + \frac{\partial P_{xy}}{\partial y}\right) = 0 \tag{14c}$$

$$\frac{\partial M_{xy}}{\partial x} + \frac{\partial M_y}{\partial y} - Q_y + 3c_1 R_y - c_1\left(\frac{\partial P_{xy}}{\partial x} + \frac{\partial P_y}{\partial y}\right) = 0 \tag{14d}$$

with k_1 is Winkler foundation modulus, k_2 is the shear layer foundation stiffness of Pasternak model.

Substituting Eq. (12) with Airy's stress function into Eq. (11), results in Eq. (114-14d) are as follows:

$$\begin{aligned} &L_{11}(W)+L_{12}(\Phi_x)+L_{13}(\Phi_y)+L_{14}(f)+L_{15}(w,f)=0\\ &L_{21}(W)+L_{22}(\Phi_x)+L_{23}(\Phi_y)+L_{24}(f)=0\\ &L_{31}(W)+L_{32}(\Phi_x)+L_{33}(\Phi_y)+L_{34}(\mathrm{f})=0 \end{aligned} \tag{15}$$

with $L_{ij}\left(i=1\div 3, j=1\div 5\right)$ that are given in Appendix.

In this work, the edges of the stiffened plates were assumed to be simply supported. Depending on the in-plane restraint at the edges, two cases of boundary conditions are considered as follows [24]:

Case 1: The edges are simply supported and freely movable. The associated boundary conditions are:

$$\begin{aligned} &w=N_{xy}=\varphi_y=M_x=P_x=0, N_x=N_{x0} \quad at \quad x=0,a\\ &w=N_{xy}=\varphi_x=M_y=P_y=0, N_y=N_{y0} \quad at \quad x=0,b \end{aligned} \tag{16}$$

Case 2: The edges are simply supported and immovable. The associated boundary conditions are:

$$\begin{aligned} &\mathrm{w}=u=\phi_y=M_x=P_x=0, \quad N_x=N_{x0} \quad at \quad x=0,\ a,\\ &\mathrm{w}=v=\phi_x=M_y=P_x=0, \quad N_y=N_{y0} \quad at \quad y=0,\ b, \end{aligned} \tag{17}$$

where N_{x0}, N_{y0} are pre-buckling compressive force resultants in directions x, y, respectively.

The approximate solutions of Eqs. (15) satisfied the boundary conditions can be determined as seen in [23]:

$$\begin{aligned} &\left(w.w^*\right)\left(x,y\right)=\left(W,\mu h\right)\sin\alpha x\sin\beta y,\\ &\phi_x\left(x,y\right)=\Phi_x\cos\alpha x\sin\beta y,\\ &\phi_y\left(x,y\right)=\Phi_y\sin\alpha x\cos\beta y,\\ &f\left(x,y\right)=A_1\cos 2\alpha x+A_2\cos 2\beta y+A_3\sin\alpha x\sin\beta y+\frac{1}{2}N_{x0}y^2+\frac{1}{2}N_{y0}x^2, \end{aligned} \tag{18}$$

in which $\alpha=m\pi/a$, $\beta=n\pi/b$, and m,n are the numbers of half waves in the x and y directions, respectively. μ is imperfection parameter of the plates, and A_1, A_2, A_3 are expressed as following:

$$A_1=\beta^2\frac{\Delta}{32B_{11}\alpha^2}W\left(W+2\mu h\right), A_2=\alpha^2\frac{\Delta}{32B_{22}\beta^2}W\left(W+2\mu h\right), A_3=\frac{H_4}{H_1}\mathrm{W}+\frac{H_2}{H_1}\Phi_x+\frac{H_3}{H_1}\Phi_y$$

Replacing solutions from Eqs. (18) into Eqs. (15) to obtain the resulting equations and then applying Galerkin method yields:

$$\begin{aligned} &l_{11}\mathrm{W}+l_{12}\Phi_x+l_{13}\Phi_y+l_{14}\Phi_x\left(\mathrm{W}+\mu h\right)+l_{15}\Phi_y\left(\mathrm{W}+\mu h\right)+l_{16}\mathrm{W}\left(\mathrm{W}+\mu h\right)\\ &+l_{17}\mathrm{W}\left(\mathrm{W}+2\mu h\right)+l_{18}\mathrm{W}\left(\mathrm{W}+\mu h\right)\left(\mathrm{W}+2\mu h\right)-\frac{ab}{4}\left(N_{x0}\alpha^2+N_{y0}\beta^2\right)\left(\mathrm{W}+\mu h\right)=0\\ &l_{21}W+l_{22}\Phi_x+l_{23}\Phi_y+l_{24}W\left(W+2\mu h\right)=0\\ &l_{31}W+l_{32}\Phi_x+l_{33}\Phi_y+l_{34}\mathrm{W}\left(\mathrm{W}+2\mu h\right)=0 \end{aligned} \tag{19}$$

in where, the detail of coefficients $l_{ij}\left(i=1\div 3, j=1\div 8\right)$ are given in Appendix.

Using the second and third equations of the Eqs. (19) system leads to:

$$\begin{aligned}\Phi_x &= \frac{l_{23}l_{31}-l_{33}l_{21}}{l_{33}l_{22}-l_{23}l_{32}}W + \frac{l_{23}l_{34}-l_{33}l_{24}}{l_{33}l_{22}-l_{23}l_{32}}W\left(\mathrm{W}+2\mu h\right)\\ \Phi_y &= \frac{l_{22}l_{31}-l_{32}l_{21}}{l_{32}l_{23}-l_{22}l_{33}}W + \frac{l_{22}l_{34}-l_{32}l_{24}}{l_{32}l_{23}-l_{22}l_{33}}\mathrm{W}\left(\mathrm{W}+2\mu h\right)\end{aligned} \tag{20}$$

3.1. Mechanical Loading

Consider a FG CNTRC plate with the edges which is simply supported and freely movable (Case 1 of boundary conditions) subjected to compressive load:

$$N_{x0} = -F_x h, N_{y0} = -F_y h \tag{21}$$

For the plate under axial compression with $F_y = 0$, the equation for the investigation of the mechanical buckling behaviour of nanocomposite plates is obtained as follows:

$$F_x = g_1\frac{\overline{\mathrm{W}}}{\left(\overline{\mathrm{W}}+\mu\right)} + g_2\overline{\mathrm{W}} + g_3\frac{\overline{\mathrm{W}}\left(\overline{\mathrm{W}}+2\mu\right)}{\left(\overline{\mathrm{W}}+\mu\right)} + g_4\overline{\mathrm{W}}\left(\overline{\mathrm{W}}+2\mu\right) \tag{22}$$

where $\overline{\mathrm{W}} = \frac{W}{h}$ and the coefficients $g_i\left(i=1-4\right)$ are given in Appendix.

3.2. Thermal loading

Consider a FG CNTRC plate with the edges supported immovably (Case 2 of boundary conditions):

$$\int_0^b\int_0^a \frac{\partial u}{\partial x}dxdy = 0, \int_0^a\int_0^b \frac{\partial v}{\partial y}dydx = 0. \tag{23}$$

From Eq. (6) one can obtain the following expression in which Eq. (12) and without imperfection of the plate:

$$\begin{aligned}\frac{\partial u}{\partial x} &= \frac{B_{22}}{\Delta}\frac{\partial^2 f}{\partial y^2} - \frac{B_{12}}{\Delta}\frac{\partial^2 f}{\partial x^2} + b_{11}\frac{\partial \phi_y}{\partial y} + b_{12}\frac{\partial \phi_x}{\partial x} + b_{13}\frac{\partial^2 w}{\partial x^2} + b_{14}\frac{\partial^2 w}{\partial y^2} - b_{15}\Phi_1\\ &- \frac{B_{28}B_{12}}{\Delta}\Phi^s_{1y} + \frac{B_{18}B_{22}}{\Delta}\Phi^s_{1x} - \frac{1}{2}\left(\frac{\partial w}{\partial x}\right)^2 - \frac{\partial w}{\partial x}\frac{\partial w^*}{\partial x},\\ \frac{\partial v}{\partial y} &= \frac{B_{11}}{\Delta}\frac{\partial^2 f}{\partial x^2} - \frac{B_{12}}{\Delta}\frac{\partial^2 f}{\partial y^2} + b_{21}\frac{\partial \phi_x}{\partial x} + b_{22}\frac{\partial \phi_y}{\partial y} + b_{23}\frac{\partial^2 w}{\partial x^2} + b_{24}\frac{\partial^2 w}{\partial y^2} - b_{25}\Phi_1\\ &- \frac{B_{18}B_{12}}{\Delta}\Phi^s_{1x} + \frac{B_{11}B_{28}}{\Delta}\Phi^s_{1y} - \frac{1}{2}\left(\frac{\partial w}{\partial y}\right)^2 - \frac{\partial w}{\partial y}\frac{\partial w^*}{\partial y},\end{aligned} \tag{24}$$

Replacing $\frac{\partial u}{\partial x}$ and $\frac{\partial v}{\partial y}$ from Eqs. (24) into Eq. (23), one can have:

$$N_{x0} = c_{11}\Phi_x + c_{12}\Phi_y + c_{13}\mathrm{W} + c_{14}\mathrm{W}^2 + c_{15}\mathrm{W}\mu h + c_{16}\Phi_1 + c_{17}\Phi^s_{1x}, \tag{25a}$$

$$N_{y0} = c_{21}\Phi_x + c_{22}\Phi_y + c_{23}\mathrm{W} + c_{24}\mathrm{W}^2 + c_{25}\mathrm{W}\mu h + c_{26}\Phi_1 + c_{27}\Phi_{1y}^s, \quad (25b)$$

Introduction of Eqs. (25) and (20) into the first of the system of Eqs. (19) taking into account temperature increment ΔT in Eq. (7), one can obtain an equation for the thermal buckling behaviour of the nanocomposite plate:

$$\Delta T = e_1 \frac{\overline{\mathrm{W}}}{\left(\overline{\mathrm{W}} + \mu\right)} + e_2 \overline{\mathrm{W}} + e_3 \frac{\overline{\mathrm{W}}\left(\overline{\mathrm{W}} + 2\mu\right)}{\left(\overline{\mathrm{W}} + \mu\right)} + e_4 \overline{\mathrm{W}}\left(\overline{\mathrm{W}} + 2\mu\right) + e_5 \overline{\mathrm{W}}^2 + e_6 \overline{\mathrm{W}}\mu, \quad (26)$$

with the coefficients $e_i \left(i = 1 \div 6\right)$ given in Appendix.

3.3. Combined Mechanical and Thermal Loading

Substituting $N_{x0} = -F_x h$, Eq. (25a) and Eq. (20) into the first of the system of Eqs. (19), one can obtain an equation for the mechanical - thermal buckling behaviour of nanocomposite plates:

$$F_x = j_1 \frac{\overline{\mathrm{W}}}{\left(\overline{\mathrm{W}} + \mu\right)} + j_2 \overline{\mathrm{W}} + j_3 \frac{\overline{\mathrm{W}}\left(\overline{\mathrm{W}} + 2\mu\right)}{\left(\overline{\mathrm{W}} + \mu\right)} + j_4 \overline{\mathrm{W}}\left(\overline{\mathrm{W}} + 2\mu\right) + j_5 \overline{\mathrm{W}}^2 + j_6 \overline{\mathrm{W}}\mu + j_7 \Delta T \quad (27)$$

with the coefficients $j_i \left(i = 1 \div 7\right)$ that are given in Appendix.

4. Results and Discussion

4.1. Comparison

To validate the method in this work, a comparison is carried out for the critical buckling load $P_{cr}(kN)$ of the FG CNTRC plates with Shen's results. Table 2 shows that the obtained results are good agreement with those reported in [7].

Table 2. Comparison of the critical buckling load $P_{cr}(kN)$ of the FG CNTRC plates without stiffeners ($a/b = 1.0, b/h = 20, h = 2mm$)

ΔT	$V_{CN}^* = 0.12$		$V_{CN}^* = 0.17$		$V_{CN}^* = 0.28$	
	Ref. [7]	Present study	Ref. [7]	Present study	Ref. [7]	Present study
The edges are simply supported and freely movable						
300K	13.04	13.55	19.91	20.06	28.69	29.36
500K	11.54	12.10	17.74	18.23	25.22	24.31
700K	9.54	10.36	14.84	15.84	20.51	21.36
The edges are simply supported and immovable						
300K	12.91	13.23	19.70	20.76	28.48	27.98
500K	9.95	10.39	15.16	16.34	22.63	23.67
700K	4.95	5.08	7.75	8.23	13.95	14.09

4.2. Mechanical Loading Analysis

In this section, numerical results are presented for the nonlinear mechanical buckling and post-buckling behaviour of FG-CNTRC plates. The detailed geometrical parameters of the FG CNTRC plates are shown in each figure.

Table 3 presents the effect of volume fractions and types of distribution of CNTs on the critical buckling load of the nanocomposite plates. As can be seen, the value of the critical buckling load increases when CNT volume fraction increases. This can be explained as follows. The volume fraction of CNTs increases, resulting in the increase of both the stiffness and buckling coefficient, since the stiffness of CNTs is much larger than the stiffness of the surrounding matrix. Moreover, the critical buckling load of the plates in the case of FG-X distribution is the largest among three case of CNT's distribution.

Figures 2 and 3 present the effect of volume fractions and types of distribution of CNTs on the load-deflection curves of the nanocomposite plates, respectively. The same conclusion with the results of the critical buckling load, the load-deflection curves of the nanocomposite plates increase when CNTs volume fraction increases. Thus, the mechanical post-buckling strength of the FG-X CNT reinfoced by stiffened composite plates is the largest. Whereas this value is the smallest in the case FG-O CNT's distribution.

Table 3. Effect of volume fractions of CNTs on the critical buckling load $P_{cr}(GPa)$ of the FG CNTC plates

	$V_{CN}^{*} = 0.12$	$V_{CN}^{*} = 0.17$	$V_{CN}^{*} = 0.28$
UD	0.1547	0.2342	0.3409
FG-X	0.2034	0.3096	0.4399
FG-V	0.1173	0.1765	0.2595

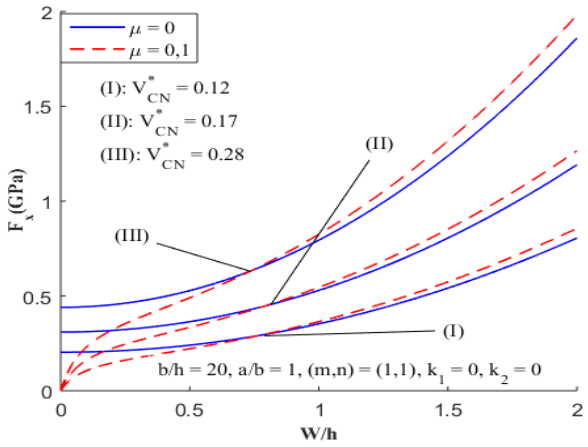

Figure 2. Effect of CNT's volume fractions on the load-deflection curves of the stiffened nanocomposite plates subjected to mechanical loading.

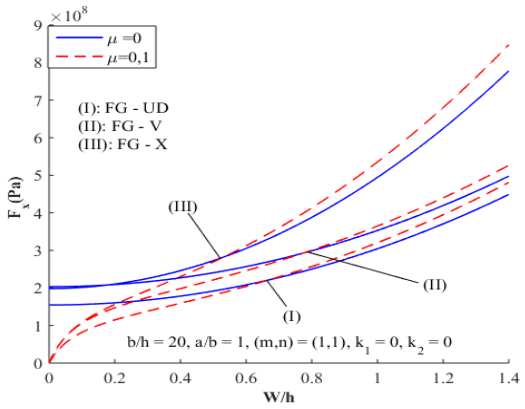

Figure 3. Effect of various types of CNT's distribution on the load-deflection curves of the stiffened nanocomposite plates subjected to mechanical loading.

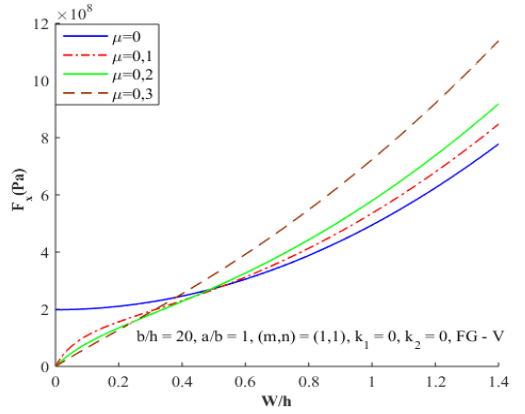

Figure 4. Effect of imperfection on the load-deflection curves of the stiffened nanocomposite plates subjected to mechanical loading.

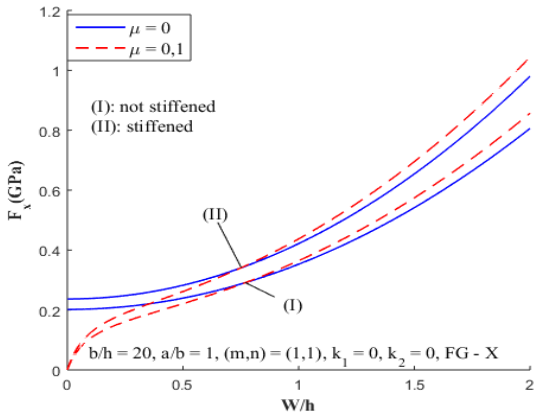

Figure 5. Effect of stiffeners on the load-deflection curves of the stiffened nanocomposite plates subjected to mechanical loading.

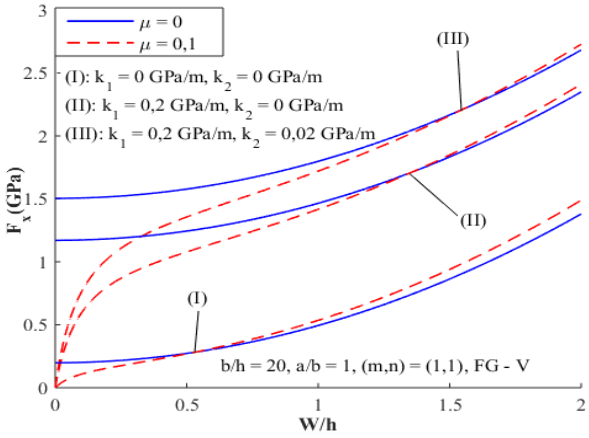

Figure 6. Effect of the foundation model on the load-deflection curves of the stiffened nanocomposite plates subjected to mechanical loading.

Figure 4 presents the influence of imperfection ($\mu = 0, 0.1, 0.2, 0.3$) of the initial shape on the load-deflection curves of the stiffened nanocomposite plates subjected to mechanical loading. It is shown that the imperfect properties have strongly affected the post-buckling strength in the limit of large enough.

Figure 5 compares the post-buckling strength of the FG CNTRC plates subjected to mechanical loading with and without stiffeners. As can see that in both cases of the perfection (μ = 0) and imperfection (μ = 0.1), the post-buckling mechanical strength of the nanocomposite plates reinforced by stiffeners is larger than that of the nanocomposite plates without stiffeners.

Figure 6 shows the effect of the elastic foundation on the load-deflection curves of the stiffened nanocomposite plates. The plate is considered resting on Winkler' elastic foundation ($k_1 \neq 0, k_2 = 0$) Pasternak's elastic foundation ($k_1 \neq 0, k_2 \neq 0$) and without elastic foundation ($k_1 = k_2 = 0$). It is shown that the foundation stiffness has a positive effect, favouring the capacity load of the FG CNTRC plates be better and the capacity load of the plates reinforced by CNTs increases when foundation stiffness increases.

4.3. Thermal Loading Analysis

Figure 7 presents the width/thicknees (b/h) ratio effect of the post-buckling behaviour of the stiffened nanocomposite plates. It is found that when b/h ratio is increased, the thermal post-buckling load-deflection curve becomes lower, and vice versa. The post-buckling curve represents the post-buckling strength of the plates so the thermal post-buckling strength of the plates decreases when ratio b/h increases

Figure 8 illustrates the effect of imperfection on the load-deflection curves of the stiffened nanocomposite plates subjected to thermal loading. As can be seen, the thermal post-buckling behaviour is affected by imperfection of the nanocomposite plates.

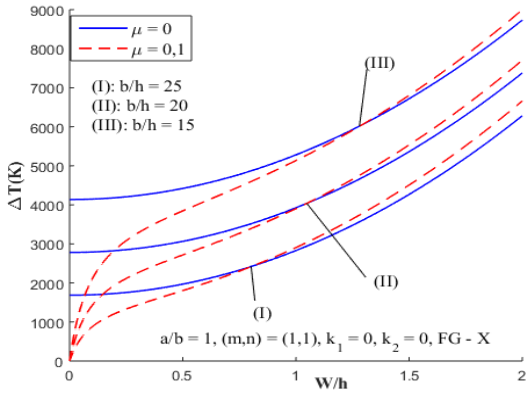

Figure 7. Effect of width to thickness ratio on the load-deflection curves of the stiffened nanocomposite plates subjected to thermal loading.

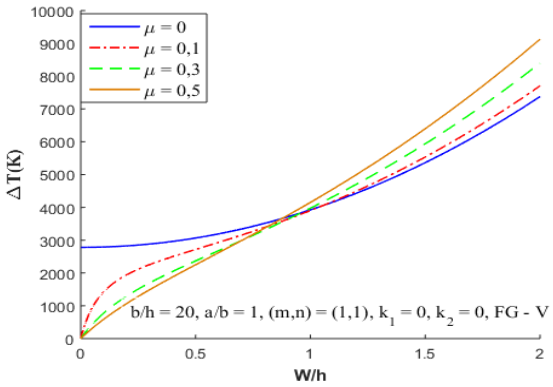

Figure 8. Effect of imperfection on the load-deflection curves of the stiffened nanocomposite plates subjected to thermal loading.

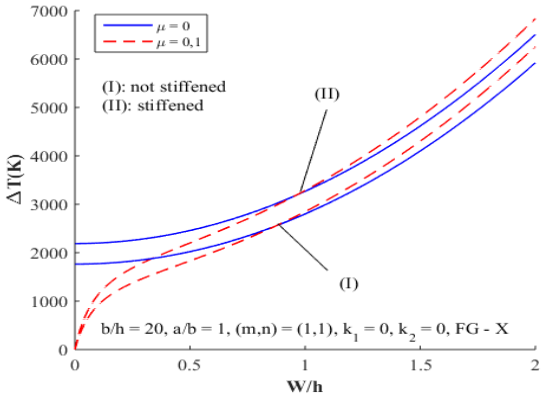

Figure 9. Effect of stiffeners on the load-deflection curves of the stiffened nanocomposite plates subjected to thermal loading.

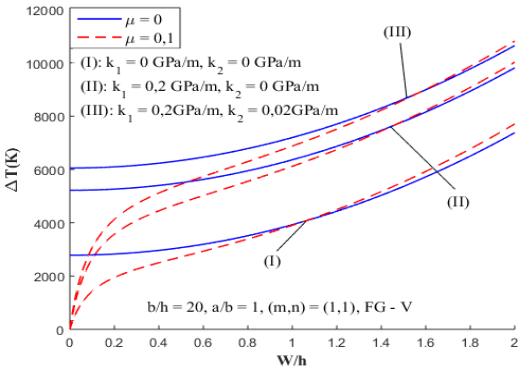

Figure 10. Effect of foundation model on the thermal post-buckling behaviour of the stiffened nanocomposite plates.

Figure 9 shows effect of stiffeners on the load-deflection curves of the stiffened nanocomposite plates subjected to thermal loading. It can be seen that the thermal post-buckling strength of the nanocomposite plates reinforced by stiffeners is higher than the one of the nanocomposite plates without stiffeners.

Figure 10 compares influences of Winker foundation model and Pasternak foundation model on the thermal post-buckling behaviour of the FG CNTRC plates. The plates are examined with three cases: without elastic foundations ($k_1 = k_2 = 0$), the Winkler foundation model ($k_1 \neq 0, k_2 = 0$), and the Pasternak foundation model ($k_1 \neq 0, k_2 \neq 0$). It can be seen that the elastic foundations have significantly affected help the thermal post-buckling strength become stronger.

4.4. Combined Loading Analysis

Numerical results are presented in this section for the nonlinear buckling and post-buckling behaviour of the stiffened nanocomposite plates subjected to thermal-mechanical loading. The influences of various types of distribution and volume fractions of carbon nanotubes on the buckling and post-buckling behaviour are shown in Table 4 and Figures 11-12, respectively. As can be seen, the effect of these factors on the stiffened nanocomposite plates for the case combined thermal loading and mechanical loading are same with results in the case the plates subjected to thermal loading or mechanical loading. Figure 13 illustrates the effects of varying temperature on the post-buckling behaviour of the stiffened nanocomposite plates subjected to thermal-mechanical loading. It seems that temperature makes the loading capacity of both perfect and imperfect plates become worse.

Table 4. Effect of volume fractions of CNTs and three types of CNTs on the critical buckling load $P_{cr}(GPa)$ of the FG CNTRC plates subjected to thermal-mechanical loading

	$V^*_{CNT} = 0.12$	$V^*_{CNT} = 0.17$	$V^*_{CNT} = 0.28$
UD	0.1286	0.1935	0.3005
FG - X	0.1767	0.2678	0.3987
FG - V	0.0915	0.1362	0.2193

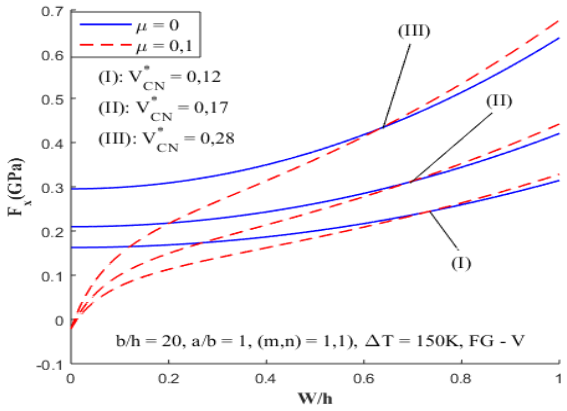

Figure 11. Effect of volume fractions of CNTs on the load-deflection of the stiffened nanocomposite plates subjected to thermal-mechanical loading.

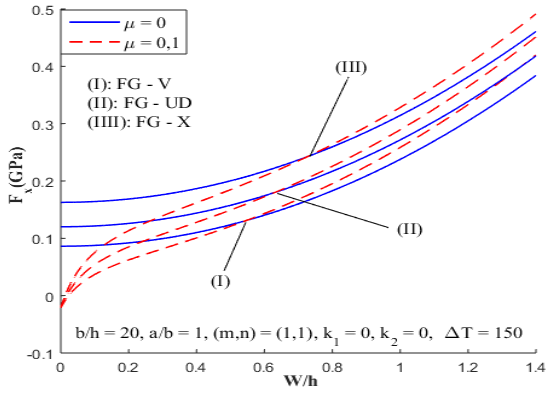

Figure 12. Effect of three types of CNTs on the load-deflection of the stiffened nanocomposite plates subjected to thermal-mechanical loading.

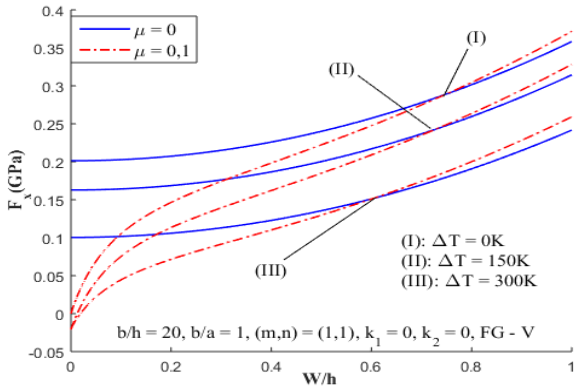

Figure 13. Effect of the temperature field on the load-deflection curves of the stiffened nanocomposite plates subjected to thermal-mechanical loading.

5. Conclusion

Some results obtained from our work are following:

- The buckling and post-buckling strength of the FG CNTRC plates subjected to mechanical loading, thermal loading and both are strongly influenced by various types of CNTs distributions. For the FG-X CNT reinfoced composite plates they exhibited the best .

- Carbon nanotubes enhanced the stiffness of the nanocomposite plates. With the increase of CNT volume fraction,the plates possess the better load capacity.

- The buckling and post-buckling strength of the stiffened nanocomposite plates subjected to various types of loads resting on Pasternak's elastic foundation is larger than the one for the plate resting on Winkler's elastic foundation and the plate without elastic foundation.

- The stiffeners have affected on the buckling and post-buckling behaviour of FG CNTRC plates. Specifically, the value of buckling and post-buckling strength of the plates reinforced by stiffeners is better than that of the plates without stiffeners.

- The material properties depending on temperature have an obvious impact on the nonlinear buckling behaviour of the FG CNTRC plates under mechanical and thermal loads.

- The geometrical parameters have significant effects on the nonlinear buckling and post-buckling behaviour of stiffened nanocomposite plates.

Acknowledgments

This research is funded by the Grant number CN.21.06 of VNU Hanoi - University of Engineering and Technology. The author is grateful for this support.

References

[1] M. Endo, S. Iijima, M. S. Dresselhaus, Carbon Nanotubes, First ed., Pergamon, 1997.

[2] A. B. Dalton, S. Collins, E. Muñoz, J. M. Razal, V. H. Ebron, J. P. Ferraris, J. N. Coleman, B. G. Kim, R. H. Baughman, Super-Tough Carbon-Nanotube Fibres, Nature, Vol. 423, No. 723, 2003, http:// doi: nature.com/articles/423703a.

[3] J. Suhr, N. Koratkar, P. Keblinski, P. Ajayan, Viscoelasticity in Carbon Nanotube Composites, Nature Materials, Vol. 4, No. 2, 2005, pp. 134-137, http://doi:10.1038/nmat1293.

[4] P. G. Collins, P. Avouris, Nanotubes for Electronics, Scientific American, Vol. 283, No. 6, 2000, pp. 62-69, http://doi: jstor.org/stable/26058971.

[5] L. P. Zanello, B. Zhao, H. Hu, R. C. Haddon, Bone Cell Proliferation on Carbon Nanotubes, Nano Lett, Vol. 6, No. 3, 2006, pp. 562-567, http://doi:10.1021/nl051861e.

[6] H. S. Shen, Nonlinear Bending of Functionally Graded Carbon Nanotube Reinforced Composite Plates in Thermal Environments, Compos. Struct, Vol. 91, No. 1, 2009, pp. 9-19, http://doi:10.1016/j.compstruct.2009.04.026.

[7] H. S. Shen, Z. H. Zhu, Buckling and Postbuckling Behavior of Functionally Graded Nanotube-Reinforced Composite Plates in Thermal Environments, CMC, Vol. 18, No. 2, 2010, pp. 155-182, http://doi: d1wqtxts1xzle7.cloudfront.net/39106668.

[8] Y. Kiani, Shear Buckling of FG-CNT Reinforced Composite Plates Using Chebyshev-Ritz Method, Compos Part B: Eng, Vol. 105, No. 15, 2016, pp. 176-187, http://doi:10.1016/j.compositesb.2016.09.001.

[9] Y. Kiani, Thermal Post-Buckling of FG-CNT Reinforced Composite Plates, Compos. Struct, Vol. 159, No. 1, 2017, pp. 299-306, http://doi:10.1016/j.compstruct.2016.09.084.

[10] L.W. Zhang, Z.X. Lei, K.M. Liew, Buckling Analysis of FG-CNT Reinforced Composite Thick Skew Plates Using an Element-Free Approach, Compos. Part B: Eng, Vol. 75, 2015, pp. 36-46, http:// doi: 10.1016/j.compositesb.2015.01.033.

[11] L. W. Zhang, K. M. Liew, Postbuckling Analysis of Axially Compressed CNT Reinforced Functionally Graded Composite Plates Resting on Pasternak Foundations Using an Element-Free Approach, Compos. Struct, Vol. 138, 2016, pp. 40-51, http://doi:10.1016/j.compstruct.2015.11.031.

[12] M. Mirzaei, Y. Kiani, Thermal Buckling of Temperature Dependent FG-CNT Reinforced Composite Plates, Meccanica, Vol. 51, No. 9, 2015, pp.2185-2201, http://doi:10.1007/s11012-015-0348-0.

[13] Y. Kiani, M. Mirzaei, Rectangular and Skew Shear Buckling of FG-CNT Reinforced Composite Skew Plates Using Ritz Method, Aerosp. Sci. Technol, Vol. 77, 2018, pp. 388-398, http://doi:10.1016/j.ast.2018.03.022.

[14] N. D. Duc, S. E. Kim, T. Q. Quan, D. T. Manh, N. H. Cuong, Nonlinear Buckling of Eccentrically Stiffened Nanocomposite Cylindrical Panels in Thermal Environments, Thin-Walled Struct, Vol. 146, 2020, pp. 106428, http://doi:10.1016/j.tws.2019.106428.

[15] K. Avramov, B. Uspensky, N. Sakhno, O. Nikonov, Transient Response of Functionally Graded Carbon Nanotubes Reinforced Composite Conical Shell With Ring-Stiffener Under The Action of Impact Loads, European Journal of Mechanics - A/Solids, Vol. 91, 2022, https://doi.org/10.1016/j.euromechsol.2021.104429.

[16] P. Maji, M. Rout, A. Karmakar, The Thermo-Elastic Vibration of Graphene Reinforced Composite Stiffened Plate With General Boundary Conditions, Struct, Vol. 33, 2021, pp. 99-112, http://doi:10.1016/j.istruc.2021.04.029.

[17] A. Davar, R. Azarafza, M. S. Fayez, S. Fallahi, J. E. Jam, Dynamic Response of a Grid-Stiffened Composite Cylindrical Shell Reinforced With Carbon Nanotubes to a Radial Impulse Load, Mech. Compos. Mater, Vol. 57, 2021, pp. 181-204, http://doi:10.1007/s11029-021-09944-3.

[18] R. Azarafza, A. Davar, M. S. Fayez, J. E. Jam, Free Vibration of Grid-stiffened Composite Cylindrical Shell Reinforced With Carbon Nanotubes, Mech. Compos, Vol. 56, 2020, pp. 505-522, http://doi:10.1007/s11029-020-09899.

[19] L. Bo, Q. Li, T. Tian, D. Wu, Y. Yu, X. Chen, W. Geo, Nonlinear Dynamic Investigation of The Perovskite Solar Cell With GPLR-FGP Stiffeners Under Blast Impact, International Journal of Mechanical Sciences, Vol. 213, 2021, http://doi: 10.1016/j.ijmecsci.2021.106866.

[20] T. Fu, Z. Chen, H. Yu, Z. Wang, X. Liu, An Analytical Study of Sound Transmission Through Stiffened Double Laminated Composite Sandwich Plates, Aerosp, Sci, Technol Vol. 82-83, 2018, pp. 92-104, http:// doi:10.1016/j.ast.2018.09.012.

[21] K. Bakshi, A Numerical Study on Nonlinear Vibrations of Laminated Composite Singly Curved Stiffened Shells, Compos. Struct, Vol. 278, 2021, https://doi.org/10.1016/j.compstruct.2021.114718.

[22] Z. Liu, J. Niu, R. Jia, Dynamic Analysis of Arbitrarily Restrained Stiffened Plate Under Moving Loads. Int. J. Mech. Sci, Vol. 200, 2021, http://doi:10.1016/j.ijmecsci.2021.106414.

[23] N. D. Duc, Nonlinear Static and Dynamic Stability of Functionally Graded Plates and Shells, Vietnam National University Press, Hanoi, 2014.

[24] D. Brush, B. O. Almroth, Buckling of Bars, Plates and Shells. Mc Graw-Hill,Vol. 42, 1975, http:// doi:10.1115/1.3423755.

Appendix

$$B_{11} = \frac{E_1}{1-v^2} + \frac{E_0 A_1^T}{s_1^T}, B_{12}\frac{vE_1}{1-v^2}, B_{13} = \frac{E_2}{1-v^2} + \frac{E_0 A_1^T z_1^T}{s_1^T}, B_{15} = \frac{E_4}{1-v^2} + \frac{E_0 A_1^T \left(z_1^T\right)^3}{s_1^T} + \frac{d_1^T \left(h_1^T\right)^3 E_0 z_1^T}{4 s_1^T},$$

$$B_{14} = \frac{vE_2}{1-v^2}, B_{16} = \frac{vE_4}{1-v^2}, B_{17} = \frac{1}{1-\nu}, B_{18} = \frac{1}{1-2\nu_s}\frac{d_1^T}{s_1^T}, B_{22} = \frac{E_1}{1-v^2} + \frac{E_0 A_2^T}{s_2^T}, B_{24} = \frac{E_2}{1-v^2} + \frac{E_0 A_2^T z_2^T}{s_2^T}$$

$$B_{26}=\frac{E_4}{1-v^2}+\frac{E_0A_2^T\left(z_2^T\right)^3}{s_2^T}+\frac{d_2^T\left(h_2^T\right)^3E_0z_2^T}{4s_2^T},B_{28}=\frac{1}{1-2\nu_s}\frac{d_2^T}{s_2^T},B_{31}=\frac{E_1}{2(1+\nu)},B_{32}=\frac{E_2}{2(1+\nu)},$$

$$B_{33}=\frac{E_4}{2(1+\nu)},B_{43}=\frac{E_3}{1-v^2}+\frac{E_0A_1^T\left(z_1^T\right)^2}{s_1^T}+\frac{E_0\left(h_1^T\right)^3d_1^T}{12s_1^T},B_{44}=\frac{vE_3}{1-v^2},B_{46}=\frac{v}{1-v^2}E_5,$$

$$B_{45}=\frac{E_5}{1-v^2}+\frac{E_0A_1^T\left(z_1^T\right)^4}{s_1^T}+\frac{E_0d_1^T\left(h_1^T\right)^3\left(z_1^T\right)^2}{2s_1^T}+\frac{E_0d_1^T\left(h_1^T\right)^5}{80s_1^T},B_{54}=\frac{1}{1-v^2}E_3+\frac{E_0A_2z_2^2}{s_2}+\frac{E_0h_2^3d_2}{12s_2}$$

$$B_{56}=\frac{1}{1-v^2}E_5+\frac{E_0A_2z_2^4}{s_2}+\frac{E_0d_2h_2^3z_2^2}{2s_2}+\frac{E_0d_2h_2^5}{80s_2},B_{71}=\frac{E_4}{1-v^2}+E_0A_1^T\left(z_1^T\right)^3+\frac{E_0z_1^Td_1^T\left(h_1^T\right)^3}{4},$$

$$B_{62}=\frac{E_3}{2(1+\nu)},B_{63}=\frac{E_5}{2(1+\nu)},B_{73}=\frac{E_5}{1-v^2}+E_0A_1^T\left(z_1^T\right)^4+\frac{E_0d_1^T\left(z_1^T\right)^2\left(h_1^T\right)^3}{2}+\frac{E_0d_1^T\left(h_1^T\right)^5}{80},$$

$$B_{75}=\frac{E_7}{1-v^2}+E_0A_1^T\left(z_1^T\right)^6+\frac{E_0d_1^T\left(h_1^T\right)^7}{448}+\frac{15E_0d_1^T\left(z_1^T\right)^4\left(h_1^T\right)^3}{12}+\frac{15E_0d_1^T\left(z_1^T\right)^2\left(h_1^T\right)^5}{80},B_{76}=\frac{vE_7}{1-v^2},$$

$$B_{82}=\frac{E_4}{1-v^2}+E_0A_2^T\left(z_2^T\right)^3+\frac{E_0z_2^Td_2^T\left(h_2^T\right)^3}{4},B_{84}=\frac{E_5}{1-v^2}+E_0A_2^T\left(z_2^T\right)^4+\frac{E_0d_2^T\left(z_2^T\right)^2\left(h_2^T\right)^3}{2}+\frac{E_0d_2^T\left(h_2^T\right)^5}{80},$$

$$B_{93}=\frac{E_7}{2(1+\nu)},B_{86}=\frac{E_7}{1-v^2}+E_0A_2^T\left(z_2^T\right)^6+\frac{E_0d_2^T\left(h_2^T\right)^7}{448}+\frac{15E_0d_2^T\left(z_2^T\right)^4\left(h_2^T\right)^3}{12}+\frac{15E_0d_2^T\left(z_2^T\right)^2\left(h_2^T\right)^5}{80}$$

$$L_{11}\left(w\right)=\left[\left(B_{31}-3c_1B_{62}\right)-3c_1\left(B_{62}-3c_1B_{63}\right)\right]\frac{\partial^2w}{\partial x^2}+\left[\left(B_{31}-3c_1B_{62}\right)-3c_1\left(B_{62}-3c_1B_{63}\right)\right]\frac{\partial^2w}{\partial y^2}$$
$$+\left(B_{71}c_1^2\frac{B_{15}B_{22}-B_{16}B_{12}}{\Delta}+B_{16}c_1^2\frac{B_{11}B_{16}-B_{15}B_{12}}{\Delta}-c_1^2B_{75}\right)\frac{\partial^4w}{\partial x^4}$$
$$+\left(B_{16}c_1^2\frac{B_{16}B_{22}-B_{26}B_{12}}{\Delta}+B_{82}c_1^2\frac{B_{11}B_{26}-B_{16}B_{12}}{\Delta}-c_1^2B_{86}\right)\frac{\partial^4w}{\partial y^4}-K_1w+K_2\nabla^2w$$
$$+\left(\begin{array}{l}B_{71}c_1^2\dfrac{B_{16}B_{22}-B_{26}B_{12}}{\Delta}+B_{16}c_1^2\dfrac{B_{11}B_{26}-B_{16}B_{12}}{\Delta}-c_1^2B_{76}+B_{16}c_1^2\dfrac{B_{15}B_{22}-B_{16}B_{12}}{\Delta}\\+B_{82}c_1^2\dfrac{B_{11}B_{16}-B_{15}B_{12}}{\Delta}-c_1^2B_{76}+4\left(c_1^2\dfrac{B_{33}^2}{B_{31}}-c_1^2B_{93}\right)\end{array}\right)\frac{\partial^4w}{\partial x^2\partial y^2}$$

$$L_{12}\left(\phi_x\right)=\left[\left(B_{31}-3c_1B_{62}\right)-3c_1\left(B_{62}-3c_1B_{63}\right)\right]\frac{\partial\phi_x}{\partial x}$$
$$+\left[\begin{array}{l}B_{71}\left(c_1^2\,\dfrac{B_{15}B_{22}-B_{16}B_{12}}{\Delta}-c_1\,\dfrac{B_{13}B_{22}-B_{14}B_{12}}{\Delta}\right)+B_{16}\left(c_1^2\,\dfrac{B_{11}B_{16}-B_{15}B_{12}}{\Delta}-c_1\,\dfrac{B_{11}B_{14}-B_{13}B_{12}}{\Delta}\right)\\+c_1B_{73}-c_1^2B_{75}\end{array}\right]\frac{\partial^3\phi_x}{\partial x^3}$$
$$+\left[\begin{array}{l}B_{16}\left(c_1^2\,\dfrac{B_{15}B_{22}-B_{16}B_{12}}{\Delta}-c_1\,\dfrac{B_{13}B_{22}-B_{14}B_{12}}{\Delta}\right)+B_{82}\left(c_1^2\,\dfrac{B_{11}B_{16}-B_{15}B_{12}}{\Delta}-c_1\,\dfrac{B_{11}B_{14}-B_{13}B_{12}}{\Delta}\right)\\+c_1B_{46}-c_1^2B_{76}+2\left[B_{33}c_1\left(c_1\,\dfrac{B_{33}}{B_{31}}-\dfrac{B_{32}}{B_{31}}\right)+B_{63}c_1-c_1^2B_{93}\right]\end{array}\right]\frac{\partial^3\phi_x}{\partial x\partial y^2}$$

$$L_{13}\left(\phi_y\right)=\left[\left(B_{31}-3c_1B_{62}\right)-3c_1\left(B_{62}-3c_1B_{63}\right)\right]\frac{\partial\phi_y}{\partial y}$$
$$+\left[\begin{array}{l}B_{71}\left(c_1^2\,\dfrac{B_{16}B_{22}-B_{26}B_{12}}{\Delta}-c_1\,\dfrac{B_{14}B_{22}-B_{24}B_{12}}{\Delta}\right)+B_{16}\left(c_1^2\,\dfrac{B_{11}B_{26}-B_{16}B_{12}}{\Delta}-c_1\,\dfrac{B_{11}B_{24}-B_{14}B_{12}}{\Delta}\right)\\+c_1B_{46}-c_1^2B_{76}+2\left[B_{33}c_1\left(c_1\,\dfrac{B_{33}}{B_{31}}-\dfrac{B_{32}}{B_{31}}\right)+B_{63}c_1-c_1^2B_{93}\right]\end{array}\right]\frac{\partial^3\phi_y}{\partial x^2\partial y}$$
$$+\left[\begin{array}{l}B_{16}\left(c_1^2\,\dfrac{B_{16}B_{22}-B_{26}B_{12}}{\Delta}-c_1\,\dfrac{B_{14}B_{22}-B_{24}B_{12}}{\Delta}\right)+B_{82}\left(c_1^2\,\dfrac{B_{11}B_{26}-B_{16}B_{12}}{\Delta}-c_1\,\dfrac{B_{11}B_{24}-B_{14}B_{12}}{\Delta}\right)\\+c_1B_{84}-c_1^2B_{86}\end{array}\right]\frac{\partial^3\phi_y}{\partial y^3}$$

$$L_{14}\left(f\right)=c_1\,\frac{B_{71}B_{22}-B_{16}B_{12}}{\Delta}\,\frac{\partial^4 f}{\partial x^2\partial y^2}+c_1\,\frac{B_{16}B_{11}-B_{71}B_{12}}{\Delta}\,\frac{\partial^4 f}{\partial x^4}+c_1\,\frac{B_{16}B_{22}-B_{82}B_{12}}{\Delta}\,\frac{\partial^4 f}{\partial y^4}$$
$$+c_1\,\frac{B_{82}B_{11}-B_{16}B_{12}}{\Delta}\,\frac{\partial^2 f}{\partial y^2\partial x^2}-2c_1\,\frac{B_{33}}{B_{31}}\,\frac{\partial^4 f}{\partial x^2\partial y^2},P\left(x,f\right)=\frac{\partial^2 f}{\partial y^2}\,\frac{\partial^2 w}{\partial x^2}-2\,\frac{\partial^2 f}{\partial x\partial y}\,\frac{\partial^2 w}{\partial x\partial y}+\frac{\partial^2 f}{\partial y^2}\,\frac{\partial^2 w}{\partial y^2}$$

$$L_{21}\left(w\right)=\left(B_{41}c_1\,\frac{B_{15}B_{22}-B_{16}B_{12}}{\Delta}-c_1B_{45}+B_{14}c_1\,\frac{B_{11}B_{16}-B_{15}B_{12}}{\Delta}-c_1\left(\begin{array}{l}B_{71}c_1\,\dfrac{B_{15}B_{22}-B_{16}B_{12}}{\Delta}\\+B_{16}c_1\,\dfrac{B_{11}B_{16}-B_{15}B_{12}}{\Delta}-c_1B_{75}\end{array}\right)\right)\frac{\partial^3 w}{\partial x^3}$$
$$+\left(\begin{array}{l}B_{41}c_1\,\dfrac{B_{16}B_{22}-B_{26}B_{12}}{\Delta}-c_1B_{46}+B_{14}c_1\,\dfrac{B_{11}B_{26}-B_{16}B_{12}}{\Delta}+\left(c_1\,\dfrac{B_{32}B_{33}}{B_{31}}-c_1B_{63}\right)2\\-c_1\left(B_{71}c_1\,\dfrac{B_{16}B_{22}-B_{26}B_{12}}{\Delta}+B_{16}c_1\,\dfrac{B_{11}B_{26}-B_{16}B_{12}}{\Delta}-c_1B_{76}+\left(c_1\,\dfrac{B_{33}^2}{B_{31}}-c_1B_{93}\right)2\right)\end{array}\right)\frac{\partial^3 w}{\partial x\partial y^2}$$
$$-\left[3c_1\left(B_{62}-3c_1B_{63}\right)+\left(B_{31}-3c_1B_{62}\right)\right]\frac{\partial w}{\partial x}$$

$$L_{22}\left(\phi_x\right)=-\left[3c_1\left(B_{62}-3c_1B_{63}\right)+\left(B_{31}-3c_1B_{62}\right)\right]\phi_x+\frac{\partial^2\phi_x}{\partial x^2}$$
$$\left[\begin{array}{l}B_{14}\left(c_1\dfrac{B_{11}B_{16}-B_{15}B_{12}}{\Delta}-\dfrac{B_{11}B_{14}-B_{13}B_{12}}{\Delta}\right)+B_{41}\left(c_1\dfrac{B_{15}B_{22}-B_{16}B_{12}}{\Delta}-\dfrac{B_{13}B_{22}-B_{14}B_{12}}{\Delta}\right)+B_{43}-c_1B_{45}\\ -c_1\left[B_{71}\left(c_1\dfrac{B_{15}B_{22}-B_{16}B_{12}}{\Delta}-\dfrac{B_{13}B_{22}-B_{14}B_{12}}{\Delta}\right)+B_{16}\left(c_1\dfrac{B_{11}B_{16}-B_{15}B_{12}}{\Delta}-\dfrac{B_{11}B_{14}-B_{13}B_{12}}{\Delta}\right)+B_{73}-c_1B_{75}\right]\end{array}\right]$$
$$+\left[B_{32}\left(c_1\frac{B_{33}}{B_{31}}-\frac{B_{32}}{B_{31}}\right)+B_{62}-c_1B_{63}-c_1\left[B_{33}\left(c_1\frac{B_{33}}{B_{31}}-\frac{B_{32}}{B_{31}}\right)+B_{63}-c_1B_{93}\right]\right]\frac{\partial^2\phi_x}{\partial y^2}$$

$$L_{23}\left(\phi_y\right)=\left[\begin{array}{l}B_{41}\left(c_1\dfrac{B_{16}B_{22}-B_{26}B_{12}}{\Delta}-\dfrac{B_{14}B_{22}-B_{24}B_{12}}{\Delta}\right)+B_{14}\left(c_1\dfrac{B_{11}B_{26}-B_{16}B_{12}}{\Delta}-\dfrac{B_{11}B_{24}-B_{14}B_{12}}{\Delta}\right)\\ +B_{44}-c_1B_{46}+B_{32}\left(c_1\dfrac{B_{33}}{B_{31}}-\dfrac{B_{32}}{B_{31}}\right)+B_{62}-c_1B_{63}\\ -c_1\left[\begin{array}{l}B_{71}\left(c_1\dfrac{B_{16}B_{22}-B_{26}B_{12}}{\Delta}-\dfrac{B_{14}B_{22}-B_{24}B_{12}}{\Delta}\right)+B_{46}-c_1B_{76}+B_{33}\left(c_1\dfrac{B_{33}}{B_{31}}-\dfrac{B_{32}}{B_{31}}\right)\\ +B_{63}-c_1B_{93}+B_{16}\left(c_1\dfrac{B_{11}B_{26}-B_{16}B_{12}}{\Delta}-\dfrac{B_{11}B_{24}-B_{14}B_{12}}{\Delta}\right)\end{array}\right]\end{array}\right]\frac{\partial^2\phi_y}{\partial x\partial y}$$

$$L_{24}\left(f\right)=\left(\frac{B_{41}B_{22}-B_{14}B_{12}}{\Delta}-c_1\frac{B_{71}B_{22}-B_{16}B_{12}}{\Delta}-\left(\frac{B_{32}}{B_{31}}-c_1\frac{B_{33}}{B_{31}}\right)\right)\frac{\partial^3 f}{\partial x\partial y^2}$$
$$+\left(\frac{B_{14}B_{11}-B_{41}B_{12}}{\Delta}-c_1\frac{B_{16}B_{11}-B_{71}B_{12}}{\Delta}\right)\frac{\partial^3 f}{\partial x^3}$$

$$L_{31}\left(w\right)=\left(\begin{array}{l}B_{14}c_1\dfrac{B_{15}B_{22}-B_{16}B_{12}}{\Delta}+B_{24}c_1\dfrac{B_{11}B_{16}-B_{15}B_{12}}{\Delta}-c_1B_{46}+2\left(c_1\dfrac{B_{32}B_{33}}{B_{31}}-c_1B_{63}\right)\\ -c_1\left(B_{16}c_1\dfrac{B_{15}B_{22}-B_{16}B_{12}}{\Delta}+B_{82}c_1\dfrac{B_{11}B_{16}-B_{15}B_{12}}{\Delta}-c_1B_{76}+2\left(c_1\dfrac{B_{33}^2}{B_{31}}-c_1B_{93}\right)\right)\end{array}\right)\frac{\partial^3 w}{\partial x^2\partial y}$$
$$+\left(\begin{array}{l}B_{14}c_1\dfrac{B_{16}B_{22}-B_{26}B_{12}}{\Delta}+B_{24}c_1\dfrac{B_{11}B_{26}-B_{16}B_{12}}{\Delta}-c_1B_{56}\\ -c_1\left(B_{16}c_1\dfrac{B_{16}B_{22}-B_{26}B_{12}}{\Delta}+B_{82}c_1\dfrac{B_{11}B_{26}-B_{16}B_{12}}{\Delta}-c_1B_{86}\right)\end{array}\right)\frac{\partial^3 w}{\partial y^3}$$
$$-\left[3c_1\left(B_{62}-3c_1B_{63}\right)+\left(B_{31}-3c_1B_{62}\right)\right]\frac{\partial w}{\partial y}$$

$$L_{32}\left(\phi_x\right)=\left[\begin{array}{l} B_{14}\left(c_1\dfrac{B_{15}B_{22}-B_{16}B_{12}}{\Delta}-\dfrac{B_{13}B_{22}-B_{14}B_{12}}{\Delta}\right)+B_{24}\left(c_1\dfrac{B_{11}B_{16}-B_{15}B_{12}}{\Delta}-\dfrac{B_{11}B_{14}-B_{13}B_{12}}{\Delta}\right) \\ +B_{44}-c_1B_{46}+B_{32}\left(c_1\dfrac{B_{33}}{B_{31}}-\dfrac{B_{32}}{B_{31}}\right)+B_{62}-c_1B_{63}-c_1\left[B_{33}\left(c_1\dfrac{B_{33}}{B_{31}}-\dfrac{B_{32}}{B_{31}}\right)+B_{63}-c_1B_{93}\right] \\ -c_1\left[\begin{array}{l} B_{16}\left(c_1\dfrac{B_{15}B_{22}-B_{16}B_{12}}{\Delta}-\dfrac{B_{13}B_{22}-B_{14}B_{12}}{\Delta}\right) \\ +B_{82}\left(c_1\dfrac{B_{11}B_{16}-B_{15}B_{12}}{\Delta}-\dfrac{B_{11}B_{14}-B_{13}B_{12}}{\Delta}\right)+B_{46}-c_1B_{76}\end{array}\right]\end{array}\right]\frac{\partial^2\phi_x}{\partial x\partial y}$$

$$L_{33}\left(\phi_y\right)=\left[\begin{array}{l} B_{14}\left(c_1\dfrac{B_{16}B_{22}-B_{26}B_{12}}{\Delta}-\dfrac{B_{14}B_{22}-B_{24}B_{12}}{\Delta}\right) \\ +B_{24}\left(c_1\dfrac{B_{11}B_{26}-B_{16}B_{12}}{\Delta}-\dfrac{B_{11}B_{24}-B_{14}B_{12}}{\Delta}\right)+B_{54}-c_1B_{56} \\ -c_1\left[\begin{array}{l} B_{16}\left(c_1\dfrac{B_{16}B_{22}-B_{26}B_{12}}{\Delta}-\dfrac{B_{14}B_{22}-B_{24}B_{12}}{\Delta}\right) \\ +B_{82}\left(c_1\dfrac{B_{11}B_{26}-B_{16}B_{12}}{\Delta}-\dfrac{B_{11}B_{24}-B_{14}B_{12}}{\Delta}\right)+B_{84}-c_1B_{86}\end{array}\right]\end{array}\right]\frac{\partial^2\phi_y}{\partial y^2}$$

$$+\left[B_{32}\left(c_1\frac{B_{33}}{B_{31}}-\frac{B_{32}}{B_{31}}\right)+B_{62}-c_1B_{63}-c_1\left[B_{33}\left(c_1\frac{B_{33}}{B_{31}}-\frac{B_{32}}{B_{31}}\right)+B_{63}-c_1B_{93}\right]\right]\frac{\partial^2\phi_y}{\partial x^2}$$

$$-\left[3c_1\left(B_{62}-3c_1B_{63}\right)+\left(B_{31}-3c_1B_{62}\right)\right]\phi_y$$

$$L_{34}\left(f\right)=\left(\frac{B_{14}B_{22}-B_{24}B_{12}}{\Delta}-c_1\frac{B_{16}B_{22}-B_{82}B_{12}}{\Delta}\right)\frac{\partial^3 f}{\partial y^3}$$

$$+\left(\frac{B_{24}B_{11}-B_{14}B_{12}}{\Delta}-c_1\frac{B_{82}B_{11}-B_{16}B_{12}}{\Delta}\right)\frac{\partial^3 f}{\partial y\partial x^2}-\left(\frac{B_{32}}{B_{31}}-c_1\frac{B_{33}}{B_{31}}\right)\frac{\partial^3 f}{\partial x^2\partial y}$$

$$b_{11}=\left(c_1\frac{B_{16}B_{22}-B_{26}B_{12}}{\Delta}-\frac{B_{14}B_{22}-B_{24}B_{12}}{\Delta}\right),b_{12}=\left(c_1\frac{B_{15}B_{22}-B_{16}B_{12}}{\Delta}-\frac{B_{13}B_{22}-B_{14}B_{12}}{\Delta}\right),$$

$$b_{13}=c_1\frac{B_{15}B_{22}-B_{16}B_{12}}{\Delta},b_{14}=c_1\frac{B_{16}B_{22}-B_{26}B_{12}}{\Delta},b_{15}=\frac{B_{12}B_{17}-B_{22}B_{17}}{\Delta},$$

$$b_{21}=\left(c_1\frac{B_{11}B_{16}-B_{15}B_{12}}{\Delta}-\frac{B_{11}B_{14}-B_{13}B_{12}}{\Delta}\right),b_{22}=\left(c_1\frac{B_{11}B_{26}-B_{16}B_{12}}{\Delta}-\frac{B_{11}B_{24}-B_{14}B_{12}}{\Delta}\right),$$

$$b_{23} = c_1 \frac{B_{11}B_{16} - B_{15}B_{12}}{\Delta}, b_{24} = c_1 \frac{B_{11}B_{26} - B_{16}B_{12}}{\Delta}, b_{25} = \frac{B_{12}B_{17} - B_{11}B_{17}}{\Delta}.$$

$$e_{11} = \left[\frac{4\alpha\left(b_{23}B_{12} + B_{11}b_{13}\right)}{ab\beta} + \frac{4\beta\left(b_{24}B_{12} + b_{14}B_{11}\right)}{\alpha ab} + \beta \frac{4}{\alpha ab}\frac{H_4}{H_1} \right], e_{12} = \left[\frac{4b_{21}B_{12} + 4b_{12}B_{11}}{\beta ab} + \beta \frac{4}{\alpha ab}\frac{H_2}{H_1} \right],$$

$$e_{13} = \left[\frac{4b_{22}B_{12} + 4B_{11}b_{11}}{\alpha ab} + \beta \frac{4}{\alpha ab}\frac{H_3}{H_1} \right], e_{14} = \left(\frac{B_{12}\beta^2}{8} + \alpha^2 \frac{B_{11}}{8} \right), e_{15} = \left(b_{25}B_{12} + b_{15}B_{11}\right),$$

$$e_{16} = B_{18}, e_{21} = \left[\left(b_{13}B_{12} + b_{23}B_{22}\right)\alpha\frac{4}{\beta} + \left(b_{14}B_{12} + b_{24}B_{22}\right)\beta\frac{4}{\alpha} + \frac{H_4}{H_1}\alpha\frac{4}{\beta} \right]\frac{1}{ab},$$

$$e_{22} = \left[\frac{H_2}{H_1}\alpha + b_{12}B_{12} + B_{22}b_{21} \right]\frac{4}{\beta}\frac{1}{ab}, e_{23} = \left[\frac{H_3}{H_1}\alpha\frac{4}{\beta} + \left(b_{11}B_{12} + B_{22}b_{22}\right)\frac{4}{\alpha} \right]\frac{1}{ab},$$

$$e_{24} = \frac{\left(B_{12}\alpha^2 + B_{22}\beta^2\right)}{8}, e_{25} = b_{15}B_{12} + b_{25}B_{22}, e_{26} = B_{28}$$

$$1^*_{11} = \begin{bmatrix} \left(-c_1^{\,2}e_{45}\right)\alpha^4\frac{ab}{4} - c_1^{\,2}e_{56}\beta^4\frac{ab}{4} + \left(-c_1^{\,2}e_{46} - 4c_1^{\,2}e_{63} - c_1^{\,2}e_{55}\right)\alpha^2\beta^2\frac{ab}{4} \\ -\left(-3c_1e_{74} - 3c_1e_{91} + 9c_1^{\,2}e_{92} + k_2\right)\alpha^2\frac{ab}{4} \\ -\left(e_{81} - 3c_1e_{82} + 1,2.B_{62} - 3,6c_1.B_{63} + k_2\right)\beta^2\frac{ab}{4} - k_1\frac{ab}{4} \end{bmatrix}$$

$$l^*_{12} = \left[\left(c_1e_{43} - c_1^{\,2}e_{45}\right)\alpha^3\frac{ab}{4} + \left(c_1e_{62} - c_1^{\,2}e_{63} - c_1^{\,2}e_{55} + c_1e_{53}\right)\alpha\beta^2\frac{ab}{4} - \left(-3c_1e_{74} - 3c_1e_{91} + 9c_1^{\,2}e_{92}\right)\alpha\frac{ab}{4} \right]$$

$$l^*_{13} = \begin{pmatrix} \left(c_1e_{54} - -c_1^{\,2}e_{56}\right)\beta^3\frac{ab}{4} + \left(c_1e_{44} - c_1^{\,2}e_{46} - 2c_1^{\,2}e_{63} + 2c_1e_{62}\right)\alpha^2\beta\frac{ab}{4} + \left(e_{72} - c_1e_{73}\right)\alpha^2\beta\frac{ab}{4} \\ -\left(e_{81} - 3c_1e_{82} - 3,6c_1B_{62} + 10,8c_1^{\,2}.B_{63}\right)\beta\frac{ab}{4} \end{pmatrix}$$

$$1^*_{21} = \left(-\left(-c_1e_{15} + c_1^{\,2}e_{45}\right)\alpha^3\frac{ab}{4} - \left(-c_1e_{16} - 2c_1e_{33} + c_1^{\,2}e_{46} + 2c_1^{\,2}e_{63}\right)\alpha\beta^2\frac{ab}{4} + \left(3c_1e_{74} + 3c_1e_{91} - 9c_1e_{92}\right)\alpha\frac{ab}{4} \right)$$

$$l^*_{22} = \begin{pmatrix} -\left(e_{13} - c_1e_{15} - c_1e_{43} - c_1^{\,2}e_{45}\right)\alpha^2\frac{ab}{4} - \left(e_{32} - c_1e_{33} - c_1e_{62} - c_1^{\,2}e_{63}\right)\frac{n^2\pi^2}{b^2}\frac{ab}{4} \\ +\left(3c_1e_{74} + 3c_1e_{91} - 9c_1^{\,2}e_{92}\right)\frac{ab}{4} \end{pmatrix}$$

$$l^*_{23} = -\left(e_{32} - c_1e_{33} + e_{14} - c_1e_{16} + c_1^{\,2}e_{46} - c_1e_{44} - c_1e_{62} + c_1^{\,2}e_{63}\right)\frac{mn\pi^2}{ab}\frac{ab}{4}$$

$$1^*_{31} = \begin{pmatrix} \left(c_1e_{26} - c_1^{\,2}e_{56}\right)\beta^3\frac{ab}{4} - \left(-2c_1e_{33} - c_1e_{25} + 2c_1^{\,2}e_{63} + c_1^{\,2}e_{55}\right)\alpha^2\beta\frac{ab}{4} \\ +\left(3c_1e_{82} - e_{81} + 3,6c_1B_{62} - 10,8c_1^{\,2}B_{63}\right)\beta\frac{ab}{4} \end{pmatrix}$$

$$l_{32}^{*} = -\left(e_{32} - c_1 e_{33} + e_{23} - c_1 e_{25} - c_1 e_{62} + c_1^{\,2} e_{63} - c_1 e_{53} + c_1^{\,2} e_{55}\right)\alpha\beta\,\frac{ab}{4}$$

$$l_{33}^{*} = \begin{pmatrix} -\left(e_{32} - c_1 e_{33} - c_1 e_{62} + c_1^{\,2} e_{63}\right)\alpha^2\,\frac{ab}{4} - \left(e_{24} - c_1 e_{26} - c_1 e_{54} + c_1^{\,2} e_{56}\right)\beta^2\,\frac{ab}{4} \\ +\left(3c_1 e_{82} - e_{81} + 3,6 c_1 B_{62} - 10,8 c_1^{\,2} B_{63}\right)\frac{ab}{4} \end{pmatrix}$$

$$l_{11} = \left(1^{*}_{11} + \left(c_1 e_{42}\alpha^4\,\frac{ab}{4} + c_1 e_{51}\beta^4\,\frac{ab}{4} + \left(c_1 e_{41} - 2c_1 e_{61} + c_1 e_{52}\right)\alpha^2\beta^2\,\frac{ab}{4}\right)\frac{H_4}{H_1}\right)$$

$$l_{12} = \left(l^{*}_{12} + \left(c_1 e_{42}\alpha^4\,\frac{ab}{4} + c_1 e_{51}\beta^4\,\frac{ab}{4} + \left(c_1 e_{41} - 2c_1 e_{61} + c_1 e_{52}\right)\alpha^2\beta^2\,\frac{ab}{4}\right)\frac{H_2}{H_1}\right)$$

$$l_{13} = \left(l^{*}_{13} + \left(c_1 e_{42}\alpha^4\,\frac{ab}{4} + c_1 e_{51}\beta^4\,\frac{ab}{4} + \left(c_1 e_{41} - 2c_1 e_{61} + c_1 e_{52}\right)\alpha^2\beta^2\,\frac{ab}{4}\right)\frac{H_3}{H_1}\right)$$

$$l_{21} = \left(1^{*}_{21} - \left(\left(e_{12} - c_1 e_{42}\right)\alpha^3\,\frac{ab}{4} + \left(e_{11} - e_{31} - c_1 e_{41} + c_1 e_{61}\right)\beta^2\alpha\,\frac{ab}{4}\right)\frac{H_4}{H_1}\right)$$

$$l_{22} = \left(l^{*}_{22} - \left(\left(e_{12} - c_1 e_{42}\right)\alpha^3\,\frac{ab}{4} + \left(e_{11} - e_{31} - c_1 e_{41} + c_1 e_{61}\right)\beta^2\alpha\,\frac{ab}{4}\right)\frac{H_2}{H_1}\right)$$

$$l_{23} = \left(l^{*}_{23} - \left(\left(e_{12} - c_1 e_{42}\right)\alpha^3\,\frac{ab}{4} + \left(e_{11} - e_{31} - c_1 e_{41} + c_1 e_{61}\right)\beta^2\alpha\,\frac{ab}{4}\right)\frac{H_3}{H_1}\right)$$

$$l_{24} = \left(e_{12} - c_1 e_{42}\right)8\alpha^3\,\frac{8}{3\alpha\beta}\,\beta^2\,\frac{\Delta}{32 B_{11}\alpha^2}$$

$$l_{31} = \left(l^{*}_{31} - \left(\left(e_{21} - c_1 e_{51}\right)\beta^3\,\frac{ab}{4} + \left(e_{22} - e_{31} + c_1 e_{61} - c_1 e_{52}\right)\alpha^2\beta\,\frac{ab}{4}\right)\frac{H_4}{H_1}\right)$$

$$l_{32} = \left(l^{*}_{32} - \left(\left(e_{21} - c_1 e_{51}\right)\beta^3\,\frac{ab}{4} + \left(e_{22} - e_{31} + c_1 e_{61} - c_1 e_{52}\right)\alpha^2\beta\,\frac{ab}{4}\right)\frac{H_2}{H_1}\right)$$

$$l_{33} = \left(l^{*}_{33} - \left(\left(e_{21} - c_1 e_{51}\right)\beta^3\,\frac{ab}{4} + \left(e_{22} - e_{31} + c_1 e_{61} - c_1 e_{52}\right)\alpha^2\beta\,\frac{ab}{4}\right)\frac{H_3}{H_1}\right), \qquad l_{34} = \left(e_{21} - c_1 e_{51}\right)\frac{2}{3}\,\alpha\,\frac{\Delta}{B_{22}}$$

$$g_1 = -\left[l_{11} + l_{12}\,\frac{l_{23}l_{31} - l_{33}l_{21}}{l_{33}l_{22} - l_{23}l_{32}} + l_{13}\,\frac{l_{22}l_{31} - l_{32}l_{21}}{l_{32}l_{23} - l_{22}l_{33}}\right]\frac{4}{abh\alpha^2}, g_2 = -\left[l_{14}\,\frac{l_{23}l_{31} - l_{33}l_{21}}{l_{33}l_{22} - l_{23}l_{32}} + l_{15}\,\frac{l_{22}l_{31} - l_{32}l_{21}}{l_{32}l_{23} - l_{22}l_{33}} + l_{16}\right]\frac{4}{ab\alpha^2}$$

$$g_3 = -\left[l_{12}\,\frac{l_{23}l_{34} - l_{33}l_{24}}{l_{33}l_{22} - l_{23}l_{32}} + l_{13}\,\frac{l_{22}l_{34} - l_{32}l_{24}}{l_{32}l_{23} - l_{22}l_{33}} + l_{17}\right]\frac{4}{ab\alpha^2}, g_4 = -\left[l_{14}\,\frac{l_{23}l_{34} - l_{33}l_{24}}{l_{33}l_{22} - l_{23}l_{32}} + l_{15}\,\frac{l_{22}l_{34} - l_{32}l_{24}}{l_{32}l_{23} - l_{22}l_{33}} + l_{18}\right]\frac{4h}{ab\alpha^2}$$

$$e_1 = \frac{1}{G_1}\left[l_{11} + l_{12}\,\frac{l_{23}l_{31} - l_{33}l_{21}}{l_{33}l_{22} - l_{23}l_{32}} + l_{13}\,\frac{l_{22}l_{31} - l_{32}l_{21}}{l_{32}l_{23} - l_{22}l_{33}}\right],$$

$$e_2 = \frac{1}{G_1}\left[\begin{array}{l} l_{14}\dfrac{l_{23}l_{31}-l_{33}l_{21}}{l_{33}l_{22}-l_{23}l_{32}} + l_{15}\dfrac{l_{22}l_{31}-l_{32}l_{21}}{l_{32}l_{23}-l_{22}l_{33}} + l_{16} \\ -\dfrac{ab}{4}\left(\left(c_{11}\alpha^2 + c_{21}\beta^2\right)\dfrac{l_{23}l_{31}-l_{33}l_{21}}{l_{33}l_{22}-l_{23}l_{32}} + \left(c_{12}\alpha^2 + c_{22}\beta^2\right)\dfrac{l_{22}l_{31}-l_{32}l_{21}}{l_{32}l_{23}-l_{22}l_{33}} + \left(c_{13}\alpha^2 + c_{23}\beta^2\right)\right)h \end{array}\right],$$

$$e_3 = \frac{h}{G_1}\left[l_{12}\frac{l_{23}l_{34}-l_{33}l_{24}}{l_{33}l_{22}-l_{23}l_{32}} + l_{13}\frac{l_{22}l_{34}-l_{32}l_{24}}{l_{32}l_{23}-l_{22}l_{33}} + l_{17}\right], e_5 = -\frac{ab}{4G_1}\left(c_{14}\alpha^2 + c_{24}\beta^2\right)h^2, e_6 = -\frac{ab}{4G_1}\left(c_{15}\alpha^2 + c_{25}\beta^2\right)h^2,$$

$$e_4 = \frac{h^2}{G_1}\left[\begin{array}{l} l_{14}\dfrac{l_{23}l_{34}-l_{33}l_{24}}{l_{33}l_{22}-l_{23}l_{32}} + l_{15}\dfrac{l_{22}l_{34}-l_{32}l_{24}}{l_{32}l_{23}-l_{22}l_{33}} + l_{18} \\ -\dfrac{ab}{4}\left(\left(c_{11}\alpha^2 + c_{21}\beta^2\right)\dfrac{l_{23}l_{34}-l_{33}l_{24}}{l_{33}l_{22}-l_{23}l_{32}} + \left(c_{12}\alpha^2 + c_{22}\beta^2\right)\dfrac{l_{22}l_{34}-l_{32}l_{24}}{l_{32}l_{23}-l_{22}l_{33}}\right) \end{array}\right],$$

$$f_1 = \frac{B_{12}}{B_{11}}, f_2 = \left[\begin{array}{l} \dfrac{l_{23}l_{31}-l_{33}l_{21}}{l_{33}l_{22}-l_{23}l_{32}}\left(\dfrac{\Delta}{B_{11}}b_{21}\alpha + \dfrac{H_2}{H_1}\alpha^2 - \dfrac{B_{12}}{B_{11}}\dfrac{H_2}{H_1}\beta^2\right)\dfrac{4}{mn\pi^2} \\ +\dfrac{l_{22}l_{31}-l_{32}l_{21}}{l_{32}l_{23}-l_{22}l_{33}}\left(\dfrac{\Delta}{B_{11}}b_{22}\beta + \dfrac{H_3}{H_1}\alpha^2 - \dfrac{B_{12}}{B_{11}}\dfrac{H_3}{H_1}\beta^2\right)\dfrac{4}{mn\pi^2} \\ +\left(\dfrac{\Delta}{B_{11}}b_{23}\alpha^2 + \dfrac{\Delta}{B_{11}}b_{24}\beta^2 + \dfrac{H_4}{H_1}\alpha^2 - \dfrac{B_{12}}{B_{11}}\dfrac{H_4}{H_1}\beta^2\right)\dfrac{4}{mn\pi^2} \end{array}\right],$$

$$f_3 = \left[\begin{array}{l} \dfrac{l_{23}l_{34}-l_{33}l_{24}}{l_{33}l_{22}-l_{23}l_{32}}\left(\dfrac{\Delta}{B_{11}}b_{21}\alpha + \dfrac{H_2}{H_1}\alpha^2 - \dfrac{B_{12}}{B_{11}}\dfrac{H_2}{H_1}\beta^2\right)\dfrac{4}{mn\pi^2} \\ +\dfrac{l_{22}l_{34}-l_{32}l_{24}}{l_{32}l_{23}-l_{22}l_{33}}\left(\dfrac{\Delta}{B_{11}}b_{22}\beta + \dfrac{H_3}{H_1}\alpha^2 - \dfrac{B_{12}}{B_{11}}\dfrac{H_3}{H_1}\beta^2\right)\dfrac{4}{mn\pi^2} \end{array}\right],$$

$$f_4 = \frac{1}{8}\frac{\Delta}{B_{11}}\beta^2, f_5 = \frac{\Delta}{4B_{11}}\beta^2, f_6 = \left(\frac{\Delta}{B_{11}}b_{25} + \frac{B_{18}B_{12}}{B_{11}}E_s\alpha_s h_1 - B_{28}E_s\alpha_s h_2\right)$$

$$j_1 = -\left[l_{11} + l_{12}\frac{l_{23}l_{31}-l_{33}l_{21}}{l_{33}l_{22}-l_{23}l_{32}} + l_{13}\frac{l_{22}l_{31}-l_{32}l_{21}}{l_{32}l_{23}-l_{22}l_{33}}\right]\frac{4}{ab\left(h\alpha^2 + hf_1\beta^2\right)},$$

$$j_2 = -\left[l_{14}\frac{l_{23}l_{31}-l_{33}l_{21}}{l_{33}l_{22}-l_{23}l_{32}} + l_{15}\frac{l_{22}l_{31}-l_{32}l_{21}}{l_{32}l_{23}-l_{22}l_{33}} + l_{16} - \frac{ab}{4}f_2\beta^2\right]\frac{4}{ab\left(\alpha^2 + f_1\beta^2\right)},$$

$$j_3 = -\left[l_{12}\frac{l_{23}l_{34}-l_{33}l_{24}}{l_{33}l_{22}-l_{23}l_{32}} + l_{13}\frac{l_{22}l_{34}-l_{32}l_{24}}{l_{32}l_{23}-l_{22}l_{33}} + l_{17}\right]\frac{4}{ab\left(\alpha^2 + f_1\beta^2\right)},$$

$$j_4 = -\left[l_{14}\frac{l_{23}l_{34}-l_{33}l_{24}}{l_{33}l_{22}-l_{23}l_{32}} + l_{15}\frac{l_{22}l_{34}-l_{32}l_{24}}{l_{32}l_{23}-l_{22}l_{33}} + l_{18} - \frac{ab}{4}f_3\beta^2\right]\frac{4h}{ab\left(\alpha^2 + f_1\beta^2\right)},$$

$$j_5 = \frac{hf_4\beta^2}{\left(\alpha^2 + f_1\beta^2\right)}, j_6 = \frac{f_5\beta^2 h}{\left(\alpha^2 + f_1\beta^2\right)}, j_7 = \frac{f_6\beta^2}{\left(h\alpha^2 + hf_1\beta^2\right)}.$$